International Journal of Recent Engineering Science
ISSN: 2349-7157/ https://doi.org/10.14445/23497157/IJRES-V12I5P104

Volume 12 Issue 5, 29-35, Sep-Oct 2025

Original Article

Effects of Partial Substitution of Bromine on the Structural, Electronic, and Optical Properties of $CsPbI_3$ Insight from First Principles Calculations

Kwalar Barnabas Ngwani[1], Yerima J. Benson[2], Ahmad A. D[3]

[1,2,3]*Department of Physics, Modibbo Adama University, P.M.B. 5025, Yola, Adamawa State, Nigeria.*

[1]*Corresponding Author : kwalar.barnabas@tsuniversity.edu.ng*

Received: 10 August 2025 Revised: 28 September 2025 Accepted: 14 October 2025 Published: 30 October 2025

Abstract *- Adjusting the composition by partial substitution of halide gives a sure way of improving phase stability and fine-tuning the optoelectronic properties of fully inorganic perovskite halides. In this study, first-principles Density Functional Theory (DFT) computations with Spin–Orbit Coupling (SOC) were used to examine the impact of partial bromine integration on the optical, electronic, and structural properties of $CsPbI_3$. The enhanced $CsPbI_2Br$ structure shows a slight lattice contraction from 6.29 to 6.21 Å, compatible with the smaller ionic radius of bromine, which raises the Goldschmidt tolerance factor from 0.89 to 0.91 and thus stabilizes the cubic phase. The material therefore maintains a direct band gap of 1.68 eV at the R point, positioning it within the maximum range for single-junction solar cells. Projected density-of-states analysis shows that the valence band largely originates from I-5p and Br-4p orbitals hybridized with Pb-6s states, while the conduction band is influenced by Pb-6p orbitals, resulting in strong orbital coupling and low carrier effective masses. Optical analyses show a high static dielectric constant ($\varepsilon_1(0) = 5.8$), very high visible-light absorption ($>10^5$ cm^{-1}) and low reflectivity (<0.25), showing exceptional light-harvesting potential. An energy-loss peak at 5.1 eV corresponds to bulk plasmon excitation, and the optical conductivity is highest at 3.1 eV, indicating strong inter-band transitions. On the whole, the incorporation of bromine improves the electronic quality, optical response, and structural robustness of $CsPbI_3$, ranking $CsPbI_2Br$ as a bright and stable material for future generations of perovskite-based photovoltaic and optoelectronic applications.*

Keywords *- Density functional theory, Lattice contraction, Optoelectronic properties, Phase stability, Structural robustness.*

1. Introduction

Halide perovskites are one of the grey areas where intense research in material sciences is going on in recent times due to their low-cost production, compositional adjustability, and remarkable optoelectronic properties. Their ability to combine robustness, strong light absorption, and high charge-carrier mobility makes them usable for light-emitting applications, thermoelectric, and photovoltaic. [1,2] Among others, non-organic cesium lead halide perovskites ($CsPbX_3$, X = I, Br, Cl) have drawn special attention for their enhanced thermal and phase stability compared to Hybrid Organic–Inorganic Perovskites (HOIPs). [3] Their bandgap can be finely honed across the visible spectrum, allowing excellent control of optical and electronic properties necessary for upcoming optoelectronic devices. [4,5]

One of the most efficient ways to mastermind the performance of these materials is by the halide substitution method, which directly affects the optical absorption, electronic band dispersion, and lattice constant. Substituting iodide with bromine or chlorine allows continuous control of band gaps and stability. [6,7] Applying Density Functional Theory (DFT), Yu [6] reported that increasing bromine concentration in $CsPbI_{3-x}Br_x$ creates lattice contraction and hence the widening of bandgap from about 1.36 eV ($CsPbI_3$) to 2.23 eV ($CsPbBr_3$), which is in line with experimental results. Likewise, Wang and Han [8,9] found that bromine integration improves the phase stability of cubic $CsPbI_3$ and aids its thermoelectric performance, with room-temperature ZT values approaching 0.99. These findings emphasize bromine's twofold function in stabilizing perovskite structures and assisting their optoelectronic response.

Computational study using different exchange–correlation functionals such as mBJ, HSE06, and GGA-PBE has effectively reproduced experimental trends in these materials. [10,11] Many recent studies have centered on extreme compositions; either iodide-rich ($CsPbI_3$) or bromide-rich ($CsPbBr_3$), or ascertained the complete range of substitution in $CsPbI_{3-x}Br_x$ robust solutions. [12,13] However, the midway composition $CsPbI_2Br$, which represents partial bromine substitution, has attracted limited attention. This

compound is important because it incorporates the morphological stability of bromine-rich phases with the acceptable thin bandgap of iodine-rich ones, making it an excellent prospect for high-efficiency solar absorbers and photonic devices.

A major issue in the existing research is that studies often use different methods, making it hard to compare results. Results in the literature most times vary with the use of different exchange–correlation functionals, supercell models, and treatment of Spin–Orbit Coupling (SOC), which plays an important part in defining the bandgap of lead halide perovskites. [14,15] This discrepancy makes it difficult to have a clear understanding of how partial bromine substitution affects the structural and hence optoelectronic interplay in $CsPbI_2Br$.

Therefore, this research tackles this discrepancy in knowledge by using, as a matter of fact, first-principles DFT computations to study the effects of partial bromine substitution on the structural, electronic, and optical properties of $CsPbI_3$. By sustaining steady computational requirements, including SOC treatment and convergence accuracy, this study aims to ascertain a clear interdependence between bromine merger, optical response, electronic band structure, and lattice behavior. The results are therefore expected to give a distinct insight into mixed-halide compound thin film and a guiding principle for the design of $CsPbI_2Br$-based materials for effective and stable optoelectronic applications. In this research, the exchange–correlation interactions were handled by employing the Generalized Gradient Approximation (GGA) within the Perdew–Burke–Ernzerhof (PBE) functional and the hybrid functional (HSE06) for better precision. The plane-wave basis set approach was used together with Projector Augmented-Wave (PAW) and norm-conserving pseudopotentials to explain the electron–ion interactions thoroughly. [16,17]

2. Materials and Methods

2.1. Materials

The following are the materials used in this work:

a) Dell Laptop Latitude E6530
b) Quantum espresso code version 7.4.1
c) High Performance Computer (HPC)
d) Internet router
e) Source of electricity

2.2. Methods

2.2.1. Theoretical Framework

The Kohn-Sham equation in DFT is given by

$$\left[-\frac{\hbar^2}{2m}\nabla^2 + V_{ext}(r) + V_H(r) + V_{xc}(r)\right]\psi_i(r) = \in_i \psi_i(r) \tag{1}$$

Where $V_{ext}(r)$ = external potential from nuclei, $V_H(r)$ = Hartree potential and $V_{xc}(r)$ = exchange-correlation potential.

2.2.2. Optical Properties

They include dielectric function, refractive index, extinction coefficient, absorption coefficient, reflectivity, energy loss function, and optical conductivity. The dielectric function describes a material's response to an electromagnetic wave. The real part $\varepsilon_1(\omega)$ corresponds to dispersion, while the imaginary part $\varepsilon_2(\omega)$ relates to absorption. For PV materials, a high ε_2 in the visible region, it enhances light absorption, while a suitable ε_1 promotes effective screening and charge separation. [18]

The linear optical properties are obtained from the frequency-dependent complex dielectric function given by:

$$\varepsilon(\omega) = \varepsilon_1(\omega) + i\varepsilon_2(\omega) \tag{2}$$

Where ω is the photon frequency. The real part through the Kramers-Kronig relation [19] is given by

$$\varepsilon_1(\omega) = 1 + \frac{2}{\pi} P\int_0^\infty \frac{\omega'\varepsilon_2(\omega)}{\omega'^2 - \omega^2} d\omega' \tag{3}$$

$$\varepsilon_2(\omega) = \frac{8\pi^2 e^2}{\Omega}\sum_{k,v,c} |\psi_k^c | u\cdot r | \psi_k^v\rangle|^2 \ \delta\left(E_k^c - E_k^v - \hbar\omega\right) \tag{4}$$

The other optical properties were obtained using Equations 1, 2, 3, and 4.

2.2.3. Computational Details

First-principles calculations based on Density Functional Theory (DFT) were done using the Quantum ESPRESSO simulation package [20,21] to investigate the structural, electronic, and optical properties of the hybrid halide perovskite $CsPbI_2Br$. The Perdew–Burke–Ernzerhof

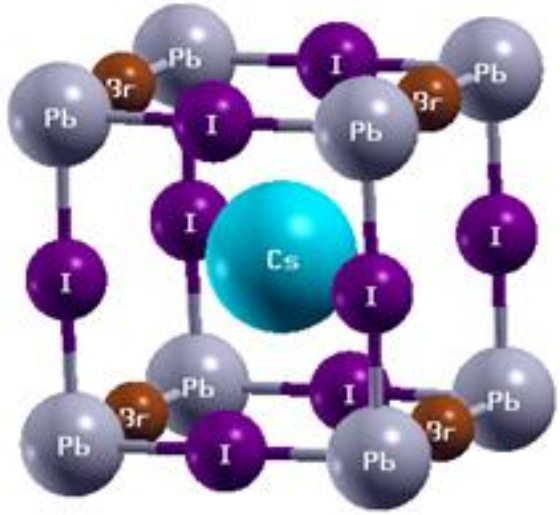

Fig. 1 Crystal Structure for $CsPbI_2Br$

(PBE) discretization of the Generalized Gradient Approximation (GGA), [17] was used to describe the exchange–correlation functional. To accurately capture relativistic effects important for systems containing heavy elements, such as Pb and I, Spin-Orbit Coupling (SOC) was specifically included in all electronic structure calculations.

Norm-conserving pseudopotentials were incorporated for Cs, Pb, I, and Br atoms; and the Kohn–Sham orbitals were expanded in a plane-wave basis set with a kinetic energy cutoff of 80 Ry, which secured the convergence of total energy and structural parameters. Brillouin zone integrations were carried out using a Monkhorst–Pack k-point mesh of 8×8×8 for Self-Consistent Field (SCF) and 16×16×16 for the Non-Self-Consistent Field (NSCF) calculations.[22] The based perovskite crystal structure was fully optimized using the variable-cell relaxation (vc-relax) method until the total energy change was less than 1×10^{-6} Ry and the Hellmann–Feynman forces on each atom were below 1×10^{-4} Ry/Bohr. Both lattice parameters and atomic positions were allowed to relax without symmetry restraints.[21,23]

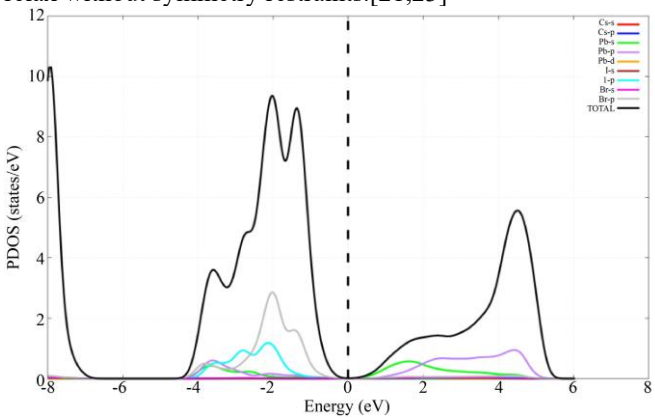

Fig. 2 Projected Density of States for $CsPbI_2Br$

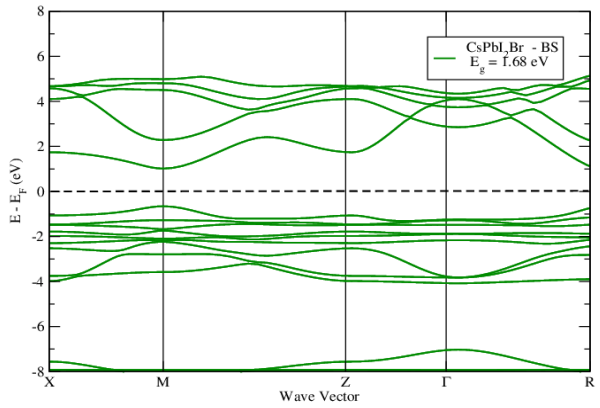

Fig. 3 Band Structure for $CsPbI_2Br$

The electronic band structure was calculated along high-symmetry paths in the Brillouin zone using the optimized lattice geometry, with SOC included self-consistently. The optical properties were calculated within the Independent Particle Approximation (IPA) using the inter-band transition matrix elements deduced from the DFT wave functions. The frequency-dependent complex dielectric function, $\varepsilon(\omega) = \varepsilon_1(\omega) + i\varepsilon_2(\omega)$, was obtained; from which derived optical constants such as refractive index, extinction coefficient, absorption coefficient, energy loss function, reflectivity, and optical conductivity were assessed. [24]

This computational order provides a balanced treatment of accuracy and computational efficiency, ensuring reliable prediction of structural, electronic, and optical properties for $CsPbI_2Br$.

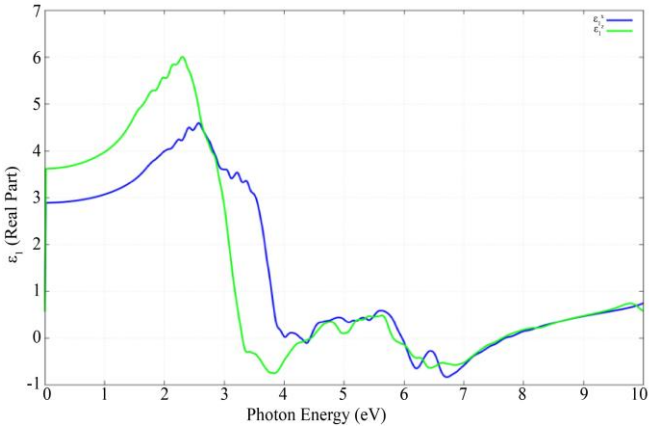

Fig. 4 Real dielectric for $CsPbI_2Br$

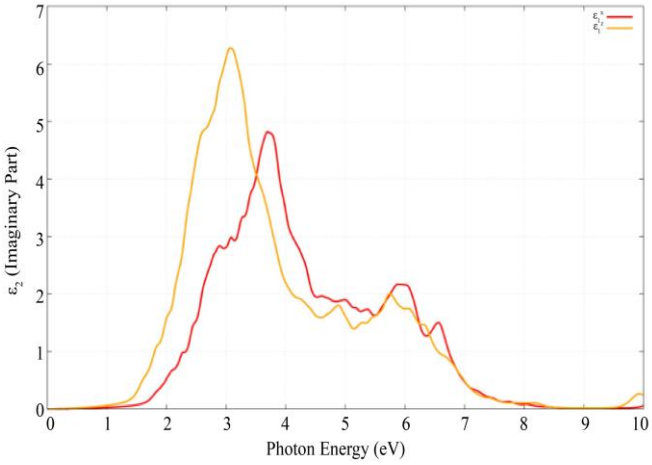

Fig. 5 Imaginary dielectric for $CsPbI_2Br$

3. Results and Discussion

3.1. Structural Properties of $CsPbI_2Br$

Figure 1 shows the optimized cubic perovskite crystal structure ($pm\bar{3}m$) of $CsPbI_2Br$, as calculated from DFT geometry optimization. In this arrangement, Pb^{2+} cations are positioned centrally within corner-sharing $[PbX_6]^{4-}$ octahedra, where X stands for the halide ions (two iodides and one bromide). Cesium cations occupy the rectified octahedron A-site voids, balancing the configuration through electrostatic interactions. [25]

3.1.1. Lattice Parameters

Upon replacing one of the iodide ions in $CsPbI_3$ with a smaller bromide ion, the improved lattice constant decreases from about 6.29 Å (pristine $CsPbI_3$) to 6.21 Å for $CsPbI_2Br$. This 1.3% contraction is consistent with the ionic radius difference between Br^- (1.96 Å) and I^- (2.20 Å). [26] This contraction increases the Goldschmidt tolerance factor (t), which is given by the formula:

$$t = \frac{r_A + r_X}{\sqrt{2}\left(r_B + r_X\right)} \tag{5}$$

Where r_A, r_B, and r_X represent the ionic radii of Cs^+, Pb^{2+}, and the halide, respectively. For $CsPbI_2Br$, t = 0.91, as

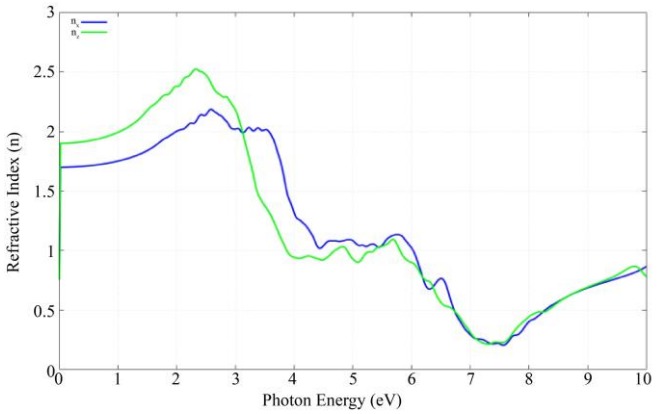

Fig. 6 Refractive Index for $CsPbI_2Br$

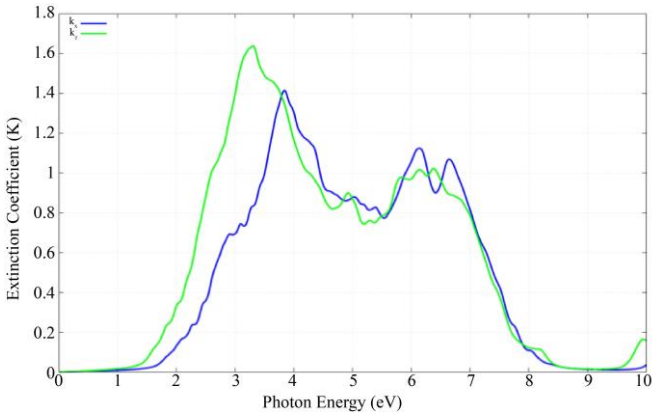

Fig. 7 The Extinction Coefficient

3.1.2. Bond Lengths and Octahedral Distortion

The Pb–I bonds in $CsPbI_2Br$ moderate 3.19 Å, whereas Pb–Br bonds reduce to about 2.95 Å, showing the smaller size and larger electronegativity of Br. This unsymmetric bonding barely varies the electronic neighborhood of the Pb^{2+} cations without noticeably deforming the octahedral coupling. The $[PbX_6]$ units stay almost perfect with bond angles close to 180°, maintaining the isotropic charge transport routes that are important for efficient photovoltaic performance. [28]

3.2. Electronic Properties $CsPbI_2Br$

The $CsPbI_2Br$'s electronic properties, as shown in Figures 2 and 3, present an explicit, semiconducting characteristic with a direct band gap found at the R point of the Brillouin zone. The computed band gap of 1.68 eV is comparable with values given in previous theoretical and experimental works on mixed halide perovskites, which often span 1.6 eV to 1.8 eV, hence asserting its relevance for single-junction photovoltaic usage, especially where maximum efficiency is taken to be near 1.5–1.7 eV. [29] The direct band gap shows that electron–hole pairs can be agitated without impurity, being an advantage for strong optical absorption in the visible spectrum.

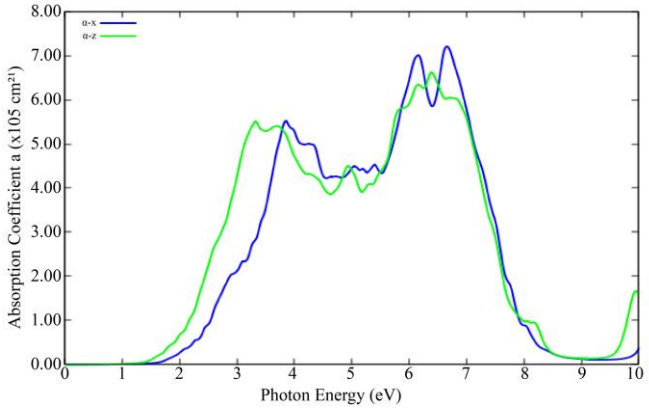

Fig. 8 Absorption Coefficient for $CsPbI_2Br$

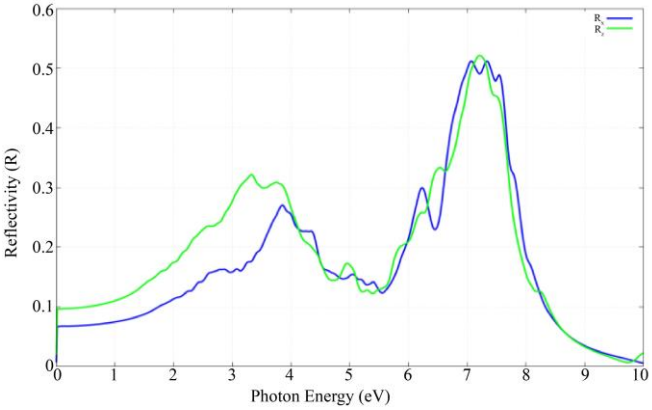

Fig. 9 Reflectivity for $CsPbI_2Br$

The Projected Density Of States (PDOS) in Figure 2 depicts that the Valence Band Maximum (VBM) is mainly formed by the halide p states; particularly, a strong hybridisation between I-5p and Br-4p orbitals with less contributions from Pb-6s states. However, the Conduction Band Minimum (CBM) is mostly made up of Pb-6p orbitals with a small mixture from halogen p states. This orbital framework is compatible with the electronic structure of lead halide perovskites, where the repulsive interplay between Pb-6p and halogen-p states orders the shape and magnitude of the band gap. [30, 31] The clear features in the PDOS close to the Fermi level also show a rather low density of trap states, which is commendable for effective carrier transport.

From the band structure in Figure 3, the dispersion of both conduction and valence bands close to the band edges is prominent, showing a small effective mass for charge carriers. This indicates high carrier mobility, which is important for decreasing recombination losses in photovoltaic devices. [32]

On the whole, the composite of a direct band gap in the maximum photovoltaic range, strong band dispersion, and clean PDOS features places $CsPbI_2Br$ as an excellent light-absorbing material for solar cells. The mixed halide makes up (I and Br), which not only affects the band gap but also clearly promotes stability, contrasted to the pure iodide match, giving a balanced concession between efficiency and durability. [33]

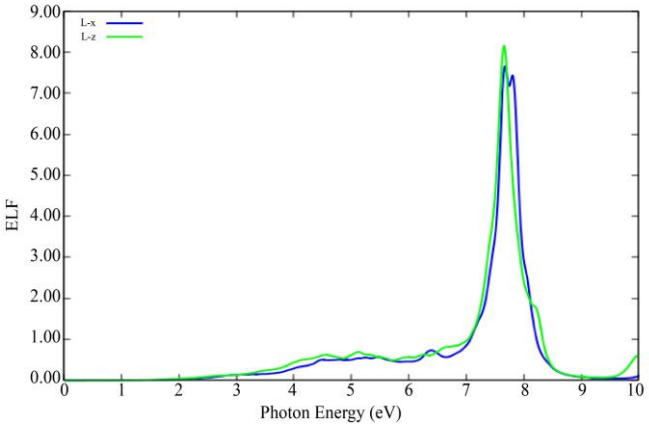

Fig. 10 Energy Loss Function for $CsPbI_2Br$

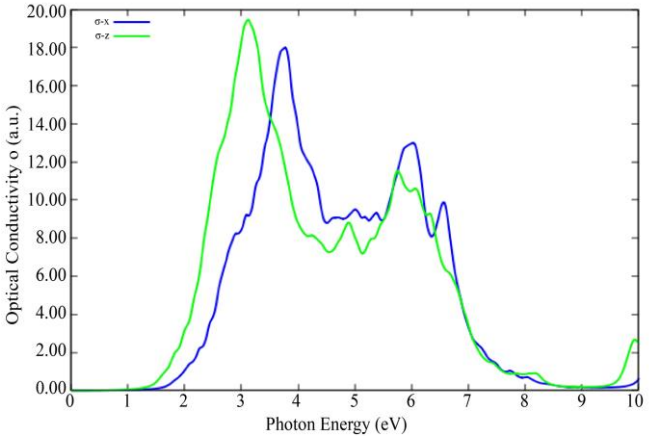

Fig. 11 Optical Conductivity for $CsPbI_2Br$

3.3. Optical Properties of $CsPbI_2Br$

The optical properties of $CsPbI_2Br$ were obtained from first-principles computations using the dielectric function protocol, and the outcomes are given in Figures 4 - 11. These properties give insight into light–matter interactions of the compound, which are crucial for its photovoltaic and optoelectronic performance. [31, 32]

3.3.1. Dielectric Function

The real part of the dielectric constant (see Figure 4) attains a peak stationary value of about $\varepsilon_1(0) = 5.8$, showing strong electronic polarizability. This suggests effective safeguarding of Coulomb interactions, which is beneficial for exciton dissolution in solar cells. The curve shows a slow decrease with photon energy, with an outstanding apex in the visible region, showing strong inter-band transitions.

The imaginary part of the dielectric constant (see Figure 5) reveals remarkable absorption peaks about 2.1 eV and 4.8 eV, comparable to direct electronic transitions from the VBM (halogen p orbitals) to the CBM (Pb-6p orbitals). The beginning of $\varepsilon_2(\omega)$ takes place near 1.9 eV, which matches well with the computed direct band gap. [32]

3.3.2. Refractive Index

The refractive index spectrum (see Figure 6) reveals a large constant value of $n(0) = 2.3$, showing strong light-bending ability, which can enhance photon confinement in thin-film devices.

The refractive index is maximum at 2.6 about 2.1 eV, coinciding with the primary $\varepsilon_2(\omega)$ peak, before gradually decreasing in the UV range. [31]

3.3.3. Extinction Coefficient

The extinction coefficient (see Figure 7) increases abruptly at the absorption edge (1.9 eV), showing the onset of notable photon absorption. It reaches its peak close to 0.8 at 2.1 eV, thus supporting the strong optical transitions in the visible range. [32]

3.3.4. Absorption Coefficient

Figure 8 indicates that $CsPbI_2Br$ shows a very high absorption coefficient surpassing 10^5 cm^{-1} across most of the visible spectrum, exceeding the threshold required for efficient solar harvesting. The absorption onset at 1.9 eV makes the material suitable for visible-light photovoltaics, while the prolonged absorption into the UV range proposes suitability for tandem or UV photo detector applications. [31]

3.3.5. Reflectivity

As shown in Figure 9, the reflectivity stays below 0.25 in the visible range, reducing light losses due to reflection. The curve is a bit maximum in the UV (0.32), in line with improved scattering at higher photon energies. [32]

3.3.6. Energy Loss Function

The energy loss function (see Figure 10) indicates a leading maximum at 5.1 eV, comparable to the bulk plasma frequency (ω_p).

This is a reflection of strong collective oscillations of free electrons at this energy, which is paramount for resolving the material's high-frequency optical characteristics. [32]

3.3.7. Optical Conductivity

Figure 11 shows that the optical conductivity increases abruptly from the peak of the band gap edge of about 3.1 eV,

comparable to the dominant inter-band transitions. This high conductivity in the visible range shows efficient photo carrier generation upon light absorption.[31]

Thus, optical analysis shows that $CsPbI_2Br$ has a direct band gap (1.9 eV), low reflectivity, high refractive index, and remarkably high absorption in the visible region. It is seen that the optical properties of $CsPbI_2Br$ are maximal on the z-axis than on the x-axis. These properties contribute to making the material a good candidate for UV-selective optoelectronic devices, top layers in tandem architectures, and single-junction solar cells. The layout between electronic structure and optical characteristics additionally underscores the relevance of $CsPbI_2Br$ for high-efficiency, stable photovoltaic applications. [32, 33]

4. Conclusion

Partially substituting bromine in $CsPbI_3$ to obtain $CsPbI_2Br$ considerably ameliorates the material's structural stability, producing a more sturdy cubic phase with a direct band gap of 1.68 eV, which is excellent for solar energy conversion. The resulting $CsPbI_2Br$ compound shows excellent visible-light absorption, strong dielectric response, and low reflectivity, making it a promising and durable candidate for high-performance perovskite solar cells and advanced optoelectronic applications.

Acknowledgement

The authors acknowledge the ICTP East African Institute for Fundamental Research for the provision of computational resources.

References

[1] Akihiro Kojima et al., "Organometal Halide Perovskites as Visible-light Sensitizers for Photovoltaic Cells," *Journal of the American Chemical Society*, vol. 131, no. 17, pp. 6050–6051, 2009. [CrossRef] [Google Scholar] [Publisher Link]

[2] Martin A. Green, Anita Ho-Baillie, and Henry J. Snaith, "The Emergence of Perovskite Solar Cells," *Nature Photonics*, vol. 8, pp. 506–514, 2014. [CrossRef] [Google Scholar] [Publisher Link]

[3] Michael Kulbak, David Cahen, and Gary Hodes, "How Important is the Organic Part of Lead Halide Perovskite Photovoltaic Cells? Efficient CsPbBr3 Cells," *Journal of Physical Chemistry Letters*, vol. 6, no. 13, pp. 2452–2456, 2015. [CrossRef] [Google Scholar] [Publisher Link]

[4] Loredana Protesescu et al., "Nanocrystals of Cesium Lead Halide Perovskites ($CsPbX_3$, X = Cl, Br, and I): Novel Optoelectronic Materials Showing Bright Emission," *Nano Letters*, vol. 15, no. 6, pp. 3692–3696, 2015. [CrossRef] [Google Scholar] [Publisher Link]

[5] Zhi-Kuang Tan et al., "Bright Light- Emitting Diodes based on Organometal Halide Perovskites," *Nature Nanotechnology*, pp. 687-692, 2014. [CrossRef] [Google Scholar] [Publisher Link]

[6] J. Yu et al., "First-Principles Study on Material Properties and Stability of Inorganic Halide Perovskite Solid Solutions $CsPb(I_{1-X}\ Br_x)_3$," *Physical Review Materials*, pp. 1-10, 2019. [CrossRef] [Google Scholar] [Publisher Link]

[7] M. Aktary, M. Kamruzzaman, and R. Afrose, "Composition-Dependent Optoelectronic Properties of $CsPbX_3$ (X = Cl, Br, Perovskites: A First-Principles Perspective," *RSC Advances*, vol. 2, pp. 23704-23717, 2022. [CrossRef] [Google Scholar] [Publisher Link]

[8] Che-Wei Lu et al., "Comparative Corrosion Behavior of Fe50Mn30Co10Cr10 Dual-phase High-entropy Alloy and CoCrFeMnNi High-entropy Alloy in 3.5 wt% NaCl Solution," *Journal of Alloys and Compounds*, vol. 842, 2020. [CrossRef] [Google Scholar] [Publisher Link]

[9] Xian Zhang et al., "Magnetic Properties of the Bulk CoFe2O4 Polycrystalline Under the Pressure," *Materials Today Communications*, vol. 28, 2021. [CrossRef] [Google Scholar] [Publisher Link]

[10] Cecilia Vona, Dmitrii Nabok, and Claudia Draxl, "Electronic Structure of (Organic-)Inorganic Metal Halide Perovskites: The Dilemma of Choosing the Right Functional," *Advanced Theory and Simulations*, vol. 5, no. 1, pp.1-11, 2022. [CrossRef] [Google Scholar] [Publisher Link]

[11] Han Chen et al., "Structure, Electronic and Optical Properties of CsPbX3 Halide Perovskite: A First-principles Study," *Computational Journal of Alloys and Compounds*, vol. 862, 2021. [CrossRef] [Google Scholar] [Publisher Link]

[12] Jueming Binget al., "Perovskite Solar Cells for Building Integrated Photovoltaics—Glazing Applications," *Joule*, vol. 6, no. 7, pp. 1446-1474, 2022. [CrossRef] [Google Scholar] [Publisher Link]

[13] Xinzheng Lan et al., "10.6% Certified Colloidal Quantum Dot Solar Cells via Solvent-Polarity-Engineered Halide Passivation," *Nano Letters*, vol. 16, no. 7, pp. 4630-4634, 2016. [CrossRef] [Google Scholar] [Publisher Link]

[14] Julia Wiktor, Ursula Rothlisberger, and Alfredo Pasquarello, "Predictive Modeling of Band Gaps in Lead Halide Perovskites: The Role of Spin–orbit Coupling," *The Journal of Physical Chemistry Letters*, vol. 8, no. 22, pp. 5507-5512, 2017. [CrossRef] [Google Scholar] [Publisher Link]

[15] Zhiyuan Huang, and Ming Lee Tang, "Semiconductor Nanocrystal Light Absorbers for Photon Upconversion," *Journal of Physical Chemistry Letters*, vol. 9, no. 21, pp. 6198-6206, 2018. [CrossRef] [Publisher Link]

[16] P.E. Blöchl, "Projector Augmented-wave Method," *Physical Review B,* 1994. [CrossRef] [Google Scholar] [Publisher Link]

[17] John P. Perdew, Kieron Burke, and Matthias Ernzerhof, "Generalized Gradient Approximation Made Simple," *Physical Review Letters,* 1996. [CrossRef] [Google Scholar] [Publisher Link]

[18] Bin Liu et al., "Optical Properties and Modeling of 2D Perovskite Solar Cells," *Solar RRL*, vol. 1, no. 8, 2017. [CrossRef] [Google Scholar] [Publisher Link]
[19] Mark Fox, *Optical Properties of Solids*, 2nd Edition, Oxford University Press, 2010. [Google Scholar] [Publisher Link]
[20] Paolo Giannozzi et al., "Quantum ESPRESSO Toward the Exascale," *The Journal of chemical physics*, vol. 152, 2020. [CrossRef] [Google Scholar] [Publisher Link]
[21] Paolo Giannozzi et al., "QUANTUM ESPRESSO: A Modular and Open-source Software Project for Quantum Simulations of Materials," *Journal of Physics: Condensed Matter*, vol. 21, no. 39, 2009. [CrossRef] [Google Scholar] [Publisher Link]
[22] Hendrik J. Monkhorst, and James D. Pack, "Special Points for Brillouin-zone Integrations," *Physical Review B,* 1976. [CrossRef] [Google Scholar] [Publisher Link]
[23] P. Giannozzi et al., "Advanced Capabilities for Materials Modeling with Quantum ESPRESSO," *Journal of Physics: Condensed Matter,* vol. 29, no. 46, 2017. [CrossRef] [Google Scholar] [Publisher Link]
[24] M. Gajdoš et al., "Linear Optical Properties in the Projector-augmented Wave Methodology," *Physical Review B*, vol. 73, 2006. [CrossRef] [Google Scholar] [Publisher Link]
[25] W.J. Yin, T. Shi, and Y. Yan, "Unique Properties of Halide Perovskites as Possible Origins of the Superior Solar Cell Performance," *Advanced Materials*, vol. 26, no. 27, pp. 4653–4658, 2014. [CrossRef] [Google Scholar] [Publisher Link]
[26] Meng-Han Wang, and Sheng-Ping Guo, "Highly Uniform Hollow CuCo2S4@C Dodecahedra Derived from ZIF-67 for High Performance Lithium-Ion Batteries," *Journal of Alloys and Compounds*, vol. 832, 2020. [CrossRef] [Google Scholar] [Publisher Link]
[27] Zhen Li et al., "Stabilizing Perovskite Structures by Tuning Tolerance Factor: Formation of Formamidinium and Cesium Lead Iodide Solid-state Alloys," *Chemistry of Materials*, vol. 28, no. 1, pp. 284-292, 2016. [CrossRef] [Google Scholar] [Publisher Link]
[28] Jingru Zhang et al., "All-inorganic $CsPbX_3$ Perovskite Solar Cells: Progress and Prospects," *Angewandte Chemie International Edition*, vol. 58, no. 44, pp. 15596-15618, 2019. [CrossRef] [Google Scholar] [Publisher Link]
[29] Chong Liu et al., "All-inorganic CsPbI2Br Perovskite Solar Cells with High Efficiency Exceeding 13%," *Journal of the American Chemical Society*, vol. 140, no. 11, pp. 3825-3828, 2018. [CrossRef] [Google Scholar] [Publisher Link]
[30] Peng-Cheng Deng et al., "First-principles Study on the Stability and Electric Properties of Zn-Doped Cspbi2Br," *SSRN*, 2025. [CrossRef] [Google Scholar] [Publisher Link]
[31] Peng Xu, "All-Inorganic Perovskite $CsPbI_2Br$ as a Promising Photovoltaic Absorber: A First-principles Study," *Journal of Chemical Sciences,* vol. 132, 2020. [CrossRef] [Google Scholar] [Publisher Link]
[32] Kailiang Yang et al., "First-principles Studies on the Structural, Electronic, Elastic, and Optical Properties of $CsPbI_2Br$ Under Pressure," *Physica Scripta,* 2025. [CrossRef] [Publisher Link]
[33] Eng Liang Lim, Jinxin Yang, and Zhanhua Wei, "Inorganic $CsPbI_2Br$ Halide Perovskite: From Fundamentals to Solar Cells Optimizations," *Energy and Environmental Science,* no. 3, 2023. [CrossRef] [Google Scholar] [Publisher Link]